

${}^4\text{He}(d,p)n{}^4\text{He}$ reaction at low bombarding energiesR. C. Luhn,* S. Sen,[†] N. O. Gaiser, and S. E. Darden*Department of Physics, University of Notre Dame, Notre Dame, Indiana 46556*

Y. Koike

Research Center for Nuclear Physics, Osaka University, Osaka 565, Japan

(Received 25 March 1985)

Cross sections, vector analyzing powers, and tensor analyzing powers were measured for the breakup reaction ${}^4\text{He}(d,p)n{}^4\text{He}$ at three bombarding energies near the 1^+ resonance in ${}^6\text{Li}$. These observables were measured to test predictions made by recent three-body calculations for this reaction in the vicinity of the 1^+ resonance. The measurements were focused on the region of the proton spectrum corresponding to the formation of the ${}^5\text{He}$ ground state. In general the three-body calculations provide a good description of the data, but discrepancies exist with T_{11} and T_{20} measurements, particularly at the lowest energy studied. The effect of the 1^+ resonance is not as pronounced in the data as in the three-body calculations, and the differences between measurements and predictions at the lowest energies seem to be a result of Coulomb effects.

INTRODUCTION

The breakup reaction $d+{}^4\text{He}\rightarrow p+n+{}^4\text{He}$ may be treated as a three-body problem provided that the deuteron bombarding energies are below about 20 MeV. In this energy range, the alpha particle may, to a good approximation, be considered a spinless, structureless boson. Renewed experimental interest in this breakup reaction in recent years has been generated by the use of three-body scattering theory to predict the observables. The success of this formalism in describing deuteron-alpha elastic scattering¹⁻³ has led to its application to the breakup problem.

Three-body calculations for observables measured in kinematically complete⁴ and incomplete⁵ experiments have shown their superiority to theoretical treatments used previously. The inability of the modified-impulse approximation to describe fully the polarization observables in kinematically incomplete experiments measuring the neutron polarization⁶ and deuteron vector-analyzing powers⁷ is a case in point. The three-body calculations have provided a much more quantitative description of the measurements.

Extensive comparisons between existing data and three-body calculations have been given in Ref. 5. In addition, predictions were made for some kinematically incomplete observables which at the time had not been measured. In particular, the polarization observables iT_{11} and T_{20} for the region of the proton spectrum corresponding to the formation of the ${}^5\text{He}$ ground state were calculated as a function of the proton detection angle and the incident beam energy in the energy region (~ 6.3 MeV) of the 1^+ resonance in ${}^6\text{Li}$. This resonance is predicted to have a strong three-body character and to affect the breakup over an energy range many times greater than the natural width of the state. The calculations show the polarization observables iT_{11} and T_{20} changing rapidly in this energy range. An interesting aspect of these predic-

tions is that the magnitude and shape of the angular distribution of T_{20} for proton energies corresponding to the formation of the ${}^5\text{He}$ ground state is due entirely to the presence of the resonance. This is interesting because the calculations included no neutron-proton tensor interaction, which is usually considered to account for tensor-analyzing power effects in (d,p) reactions. For these reasons, it was suggested that polarization data for energies near the 1^+ resonance would provide a stringent test for the three-body calculation. In addition, data at these low bombarding energies would be expected to exhibit Coulomb effects, which are not fully accounted for in the calculations.

More recent work, both experimental and theoretical, has provided new insights into this reaction. Tensor-analyzing-power measurements and three-body calculations appear in three recent reports of experiments employing kinematically complete and incomplete geometries. In a kinematically complete experiment, Slaus *et al.*⁸ measured cross sections, vector analyzing powers, and tensor analyzing powers at bombarding energies of 12 and 17 MeV. Calculations which omit the n-p tensor interaction provide a good qualitative description of the measured observables. The cross sections and vector analyzing powers are better reproduced by the calculations than are the tensor-analyzing powers. Bruno *et al.*⁹ also measured cross sections, vector analyzing powers, and tensor analyzing powers in a kinematically complete geometry at 10 MeV. The kinematical conditions were chosen to facilitate the search for the production of the isospin-forbidden n-p singlet final state. A variety of calculations were performed and compared with the data. Evidence for the n-p singlet state was inferred from fluctuations in the analyzing powers near proton energies corresponding to zero relative neutron-proton energy. However, the calculations do not reproduce these fluctuations even when the singlet n-p interaction is included.

Results from the ${}^4\text{He}(d,p)n{}^4\text{He}$ measurement at $E_d=12$

and 21 MeV by Ishikawa *et al.*¹⁰ have demonstrated both the strengths and weaknesses of the three-body calculations. The inclusion of the n-p tensor interaction in the calculation is clearly needed if the measured tensor-analyzing powers are to be reproduced by the theory. However, some discrepancies still exist between data and theory, especially for T_{20} , although the qualitative variation with proton angle and energy for this observable is reproduced. Very recently, Oswald¹¹ *et al.* published kinematically complete measurements of cross section and vector analyzing power for kinematic conditions favorable to observation of the $n\alpha$ final-state interaction at deuteron energies from 6 to 11 MeV. They have also measured an angular distribution for these observables as a function of proton c.m. angle for $E_d=7$ MeV. Their measurements are quite well reproduced by three-body calculations at the higher energies, but there exist serious discrepancies between the data and calculations for bombarding energies below 9 MeV. These recent results may be summarized by a general statement that for most observables measured, the three-body calculations provide a very good description of this breakup reaction for bombarding energies above 8 MeV.

At the time the present experiment was begun there existed no published tensor-analyzing-power data for this reaction and no polarization observables had been measured for bombarding energies less than 8 MeV. The primary motivation for the present work was a desire to test the predictions of Ref. 5 concerning both the importance of the 1^+ resonance in ${}^6\text{Li}$ and the role of the ${}^5\text{He}$ ground state production near the resonance. It was anticipated that data at these low bombarding energies might provide insight into the effects of the ${}^6\text{Li}$ 1^+ resonance and a measure of the extent of Coulomb effects.

Three energies were chosen at which to acquire data. Measurements at $E_d=5.4$, 6.0, and 6.8 MeV adequately bracket the 6.3 MeV 1^+ resonance in ${}^6\text{Li}$ and also provide data at only 1.2 MeV above the breakup threshold. The 5.4 MeV data are expected to be particularly sensitive to Coulomb effects. These three energies are also the energies for which predictions were made in Ref. 5 for iT_{11} and T_{20} . It was pointed out in Ref. 5 that the kinematically incomplete experiment ${}^4\text{He}(d,p)n$ lends itself to a study of the role of the ${}^5\text{He}$ ground state in the breakup reaction, and this was a primary motivation for our measurements. Therefore, outgoing proton energies corresponding to the formation of the ${}^5\text{He}$ ground state were the main focus of interest of the present study. Some measurements of the observables as a function of the detected proton energy are also presented, but the low bombarding energies limit the energies and angles for which such data could be obtained.

EXPERIMENTAL DETAILS

Vector and tensor-polarized deuterons were produced in the Lamb-shift polarized ion source and accelerated with the FN tandem Van de Graaff accelerator. Deuteron beams with center-of-target energies of 5.4, 6.0, and 6.8 MeV were incident on a ${}^4\text{He}$ gas target. Two different target geometries were employed. For the data at

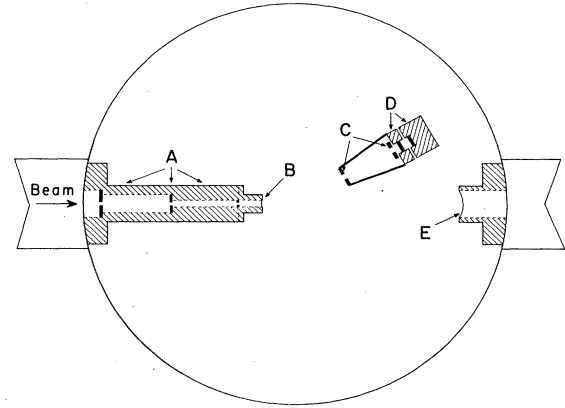


FIG. 1. Schematic diagram of the scattering chamber used for the present experiment. A depicts the beam size definition slits and antiscattering slits. B and E depict the entrance and exit foils, respectively. C depicts the detector slit system with a rectangular forward slit to define the scattering volume and a circular slit in front of the ΔE detector to define the angular acceptance. D depicts the ΔE and E detectors.

$E_d=6.8$ MeV, the target consisted of a cylindrical gas cell of radius 1.27 cm with entrance and exit foils of 2.2 μm -thick Havar foil. The pressure of the ${}^4\text{He}$ gas was approximately one atmosphere. In order to avoid the relatively large energy loss of the outgoing protons in the Havar foil for the measurements at $E_d=5.4$ and 6.0 MeV, the entire scattering chamber was filled with helium and isolated from the beam line vacuum with entrance and exit foils of 4.2 μm thick Havar. Figure 1 shows a schematic diagram of the scattering chamber geometry for this configuration. A ${}^4\text{He}$ gas pressure of 0.3 atm absolute was used.

The detector system used to identify outgoing reaction products employed two standard ΔE - E telescopes. In order to permit detection of protons at as low an energy as possible, ΔE silicon surface-barrier detectors 11 and 14 μm thick were employed. Only events in which protons traversed the ΔE detectors and stopped in the E detector were recorded in the analysis, since only in this way are

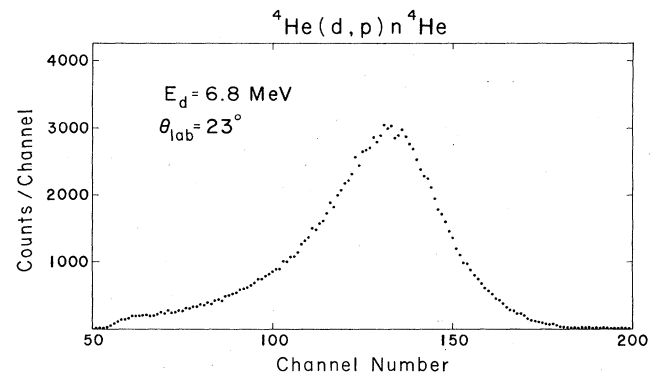


FIG. 2. A typical proton spectrum from the ${}^4\text{He}(d,p)n$ reaction. This spectrum was acquired with an unpolarized beam at $E_d=6.8$ MeV and $\theta_p=23^\circ$ for a total collected charge of 205 μC .

low-energy protons separable from low-energy alpha particles which stop in the ΔE detectors. The detector geometry is shown in Fig. 1. The slit system consisted of a rectangular forward slit 2 mm wide and a circular 3mm-diameter slit directly in front of the ΔE detector. The forward slit was positioned 2.5 cm from the target center, and the distance from the target center to the back slit was 14 cm for measurements made at laboratory angles less than 28° , and 6.4 cm otherwise. Figure 2 shows a proton spectrum taken with the experimental arrangement shown in Fig. 1. This spectrum was taken with an unpolarized beam at $E_d=6.8$ MeV and $\theta=23^\circ$ for a total charge of $205 \mu\text{C}$. The broad peak around channel 140 corresponds to the formation of the ${}^5\text{He}$ ground state. The cutoff which occurs around channel number 60 results when the protons are stopped in the ΔE detector. In calculating the polarization observables corresponding to the ${}^5\text{He}$ ground state, proton yields were obtained by summing counts over a 230-keV-wide portion of the spectrum centered on this peak.

The polarization of the beam was monitored by using a polarimeter positioned in the beam line after the scattering chamber. For the vector-polarized beam, a polarimeter based on a design of Cadmus *et al.*¹² employing the known vector-analyzing power of the ${}^4\text{He}(d,d){}^4\text{He}$ reaction was used. Typical beam polarization was $\tau_{10}=0.52\pm 0.01$ for this experiment. For the tensor-analyzing-power measurements, a tensor polarimeter utilizing the known analyzing powers of the ${}^3\text{He}(d,p){}^4\text{He}$ reaction was employed. Typical values of the tensor polarization of the beam were $\tau_{20}=-0.41\pm 0.02$.

DISCUSSION

The results of the analysis of the present measurements are presented in Figs. 3–13. In all of the figures the data appear as points with their associated uncertainties, and the curves give the results of the three-body calculations. The calculations presented employ the same potentials as were used in Ref. 5, except that the full n-p tensor interaction has been included as discussed in Ref. 10. The short-dashed curves correspond to calculations in which there is no neutron-proton tensor interaction. Solid curves correspond to calculations using a neutron-proton tensor interaction which gives rise to a deuteron d -state probability of 4%, and the long-dashed curves were calculated using a tensor force which produces a 7% deuteron d -state probability.

Figures 3 and 4 show examples of doubly differential cross sections measured at the three bombarding energies. The absolute normalization for these data was determined by the Rutherford scattering of 5.3 MeV deuterons from xenon gas using the same target and detector geometries used for the $d+{}^4\text{He}$ breakup measurements. Figure 4 shows that the ${}^5\text{He}$ ground state region of the proton spectrum has a slightly different angular distribution than that predicted by the three-body calculations.

Figure 5 presents an example of the vector-analyzing-power measurements made at 5.4 MeV as a function of proton energy in the vicinity of the ${}^5\text{He}$ ground-state peak. It can be seen that the calculations predict a much

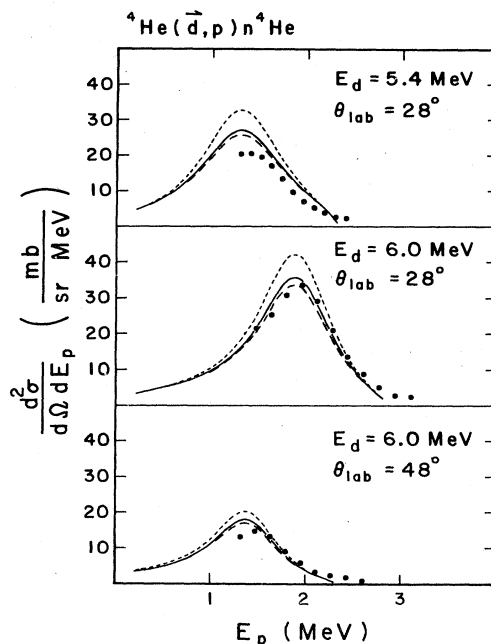


FIG. 3. Doubly differential cross sections measured at $E_d=5.4$ MeV for $\theta_p=28^\circ$ and $E_d=6.0$ MeV for $\theta_p=28^\circ$ and 48° for the top, middle, and bottom graph, respectively. The curves are the three-body calculations described in the text. The dashed curve is a three-body calculation in which there is no n-p tensor interaction. The solid and long dashed curves are three-body calculations in which the n-p tensor force gives rise to a deuteron with a D -state probability of 4% and 7%, respectively.

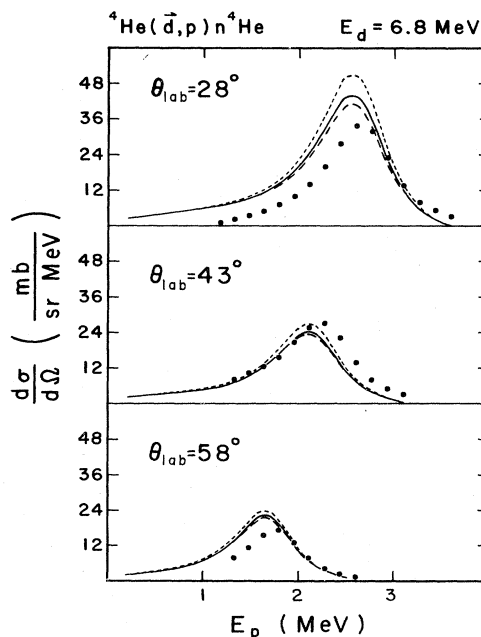


FIG. 4. Doubly differential cross sections measured at $E_d=6.8$ MeV and $\theta_p=28^\circ$, 43° , and 58° for the top, middle, and bottom graphs, respectively. The curves are the result of three-body calculations which are described in the caption for Fig. 3.

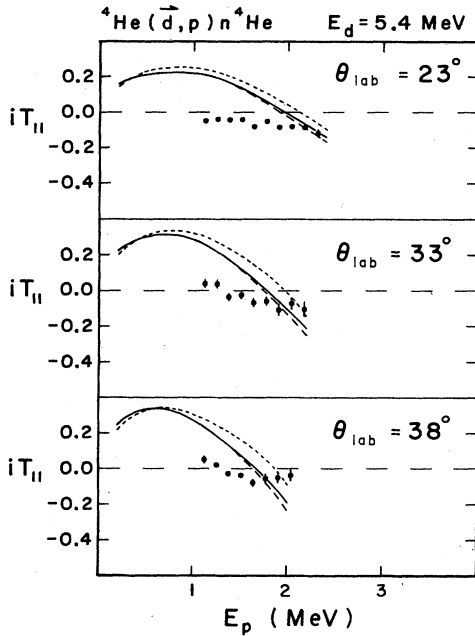


FIG. 5. The vector analyzing power for the ${}^4\text{He}(\vec{d},p)n{}^4\text{He}$ reaction as a function of the detected proton energy. The curves are the result of three-body calculations which are described in the caption for Fig. 3.

stronger energy dependence than the data exhibit.

Figures 6–8 show examples of tensor-analyzing-power measurements as a function of outgoing proton energy at the 5.4 and 6.0 MeV bombarding energies. The results are qualitatively similar for all three cases shown, and the data for T_{21} and T_{22} are reasonably well reproduced by

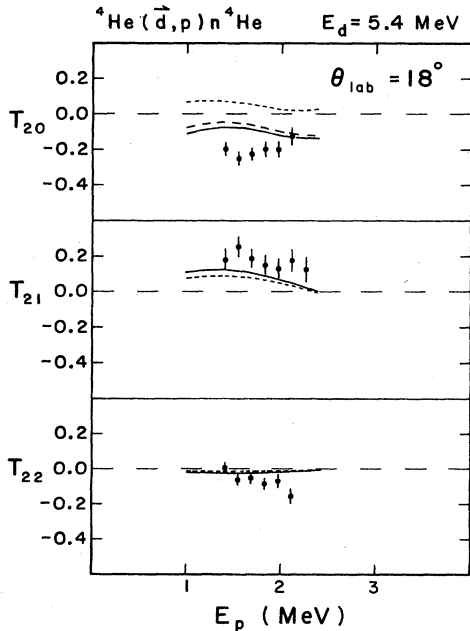


FIG. 6. The tensor analyzing powers for the ${}^4\text{He}(\vec{d},p)n{}^4\text{He}$ reaction as a function of the detected proton energy at $E_d=5.4$ MeV and $\theta_p=18^\circ$. The curves are the result of three-body calculations which are described in the caption for Fig. 3.

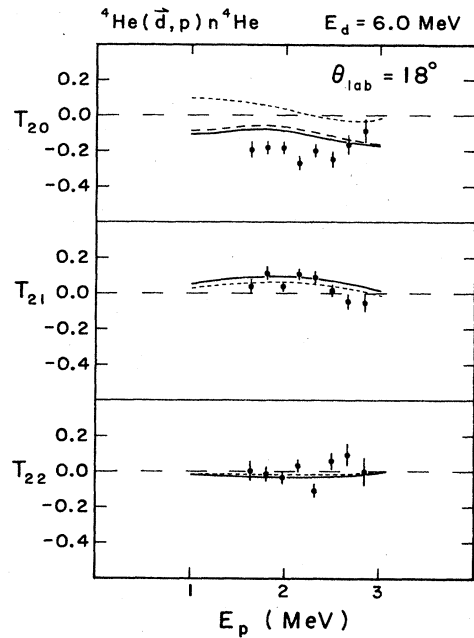


FIG. 7. The tensor analyzing powers for the ${}^4\text{He}(\vec{d},p)n{}^4\text{He}$ reaction as a function of the detected proton energy at $E_d=6.0$ MeV and $\theta_p=18^\circ$. The curves are the result of three-body calculations which are described in the caption for Fig. 3.

the calculations in all three figures. However, the T_{20} analyzing power shows at best only qualitative agreement with the calculations. Agreement between the data and calculations is best for $E_d=6.0$ MeV, where even T_{20} is fairly well reproduced. It is interesting that in these figures the T_{20} predictions agree best with experiment when

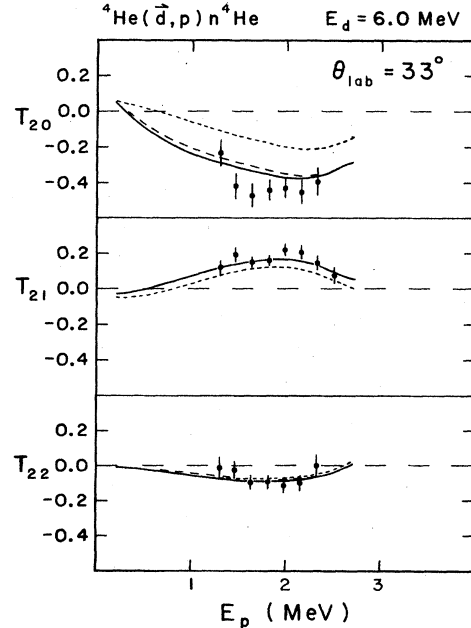


FIG. 8. The tensor analyzing powers for the ${}^4\text{He}(\vec{d},p)n{}^4\text{He}$ reaction as a function of the detected proton energy at $E_d=6.0$ MeV and $\theta_p=33^\circ$. The curves are the result of three-body calculations which are described in the caption for Fig. 3.

a neutron-proton tensor interaction is included in the calculations, although no choice between the two tensor interaction strengths can be made on the basis of these data.

The vector-analyzing powers for the formation of the ${}^5\text{He}$ ground state as a function of the proton center-of-mass angle are shown in Fig. 9. The very small values of iT_{11} at 5.4 MeV are what might be expected should the Coulomb interaction be playing a large role in the breakup at this energy. This idea is consistent with poor agreement between calculations and data at this energy, since the calculations do not properly take into account the Coulomb interaction. The increase in magnitude of iT_{11} with increasing bombarding energy may be a resonance effect. The predicted iT_{11} show a similar behavior, presumably a direct result of the 1^+ resonance in ${}^6\text{Li}$.

For deuteron energies higher than those used in the present experiment, there is evidence that the vector analyzing power for the breakup reaction proceeding through the ${}^5\text{He}$ ground state is independent of the direction along which the ${}^5\text{He}$ breaks up in its own c.m. system. For example, a comparison of the kinematically complete measurements of Oswald *et al.*¹¹ at 10 MeV for $\theta_p=50^\circ$ with the kinematically incomplete measurements of Keller and Haerberli¹³ at the same energy for $\theta_p=45^\circ$ shows the vector analyzing power to be essentially the same in both experiments. This is also predicted by the calculations.⁵ The same conclusion follows from a comparison of kinematically complete measurements of iT_{11} by Oswald *et al.* at $E_d=18$ MeV (Ref. 14) for $\theta_p=52^\circ$ with kinematically incomplete measurements carried out in our laboratory⁷ at $E_d=15$ MeV for $\theta_p=50^\circ$, since the analyzing power appears to change very little between $E_d=15$ and 18 MeV. This behavior is also predicted by the calculations. The situation is quite different for the energies used in the present measurements. Oswald *et al.*¹¹ find $A_y \approx -0.5$ in the vicinity of the ${}^5\text{He}$ peak for $\theta_p=46^\circ$ in their kinematically complete measurement at $E_d=7.0$ MeV, whereas our incomplete measurements at $E_d=6.8$ MeV as given in Fig. 9 show a much smaller analyzing power. This difference between the two experiments is also reproduced by the three-body calculations, although the agreement with the data is better for the kinematically complete measurement.

Tensor-analyzing powers for the formation of the ${}^5\text{He}$ ground state as a function of proton center-of-mass angle are shown in Figs. 11–13. Considerable similarity exists between the data at the three energies. T_{22} is everywhere small and negative. Both T_{21} and T_{22} are relatively unaffected by the change in bombarding energy, and the overall shape of T_{20} remains constant. The T_{21} and T_{22} data are well reproduced by the calculations. However, as was the case with the iT_{11} data as a function of proton energy, the T_{20} measurements are in only qualitative agreement with the calculations, since the trend of T_{20} is to decrease in magnitude with increasing bombarding energy whereas the calculations predict the opposite behavior.

One notes that there is a significant difference between the bombarding energy dependence of iT_{11} and that of the tensor analyzing powers, especially T_{20} . Whereas iT_{11} tends to zero at the lowest bombarding energies, T_{20} is

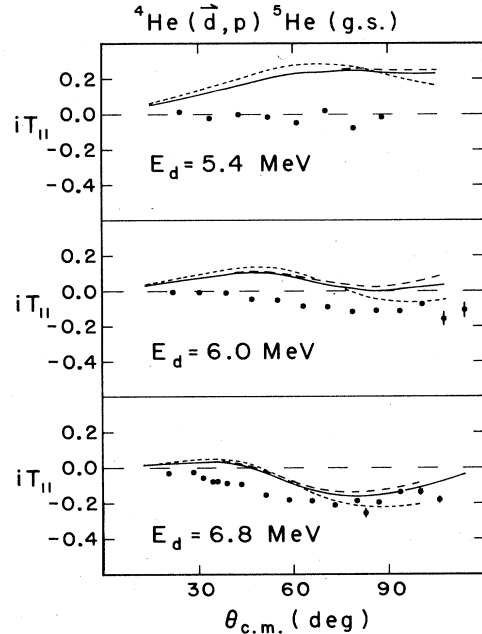


FIG. 9. The vector analyzing power for the ${}^4\text{He}(d,p){}^5\text{He}(\text{g.s.})$ reaction as a function of the proton center-of-mass angle at $E_d=5.4, 6.0,$ and 6.8 MeV for the top, middle, and bottom sections, respectively. The curves are the result of three-body calculations which are described in the caption for Fig. 3.

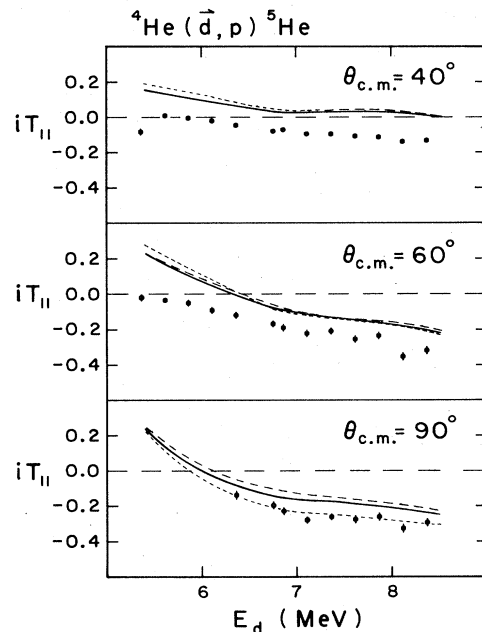


FIG. 10. The vector analyzing power for the ${}^4\text{He}(d,p){}^5\text{He}(\text{g.s.})$ reaction as a function of the deuteron bombarding energy for proton center-of-mass angles of $40^\circ, 60^\circ,$ and 90° for the top, middle, and bottom sections, respectively. The curves are the result of three-body calculations which are described in the caption for Fig. 3.

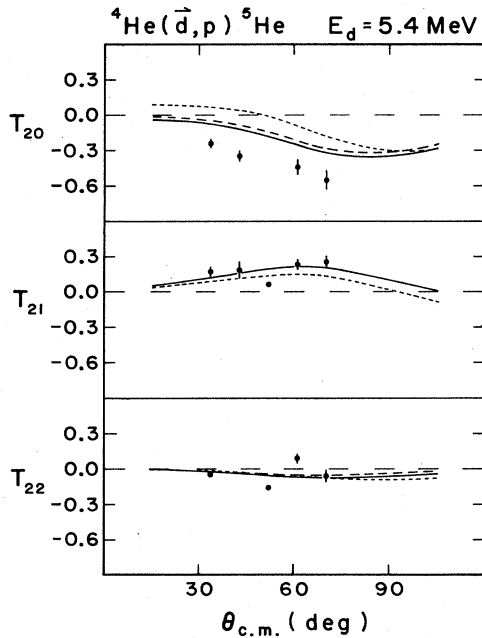


FIG. 11. The tensor analyzing powers for the ${}^4\text{He}(d,p){}^5\text{He}(\text{g.s.})$ reaction as a function of the proton center-of-mass angle at $E_d=5.4$ MeV. The curves are the result of three-body calculations which are described in the caption for Fig. 3.

largest at $E_d=5.4$ MeV. If the Coulomb interaction alone were responsible for the energy dependence of the analyzing powers, one would not expect such a pronounced difference between the behavior of iT_{11} and T_{20} .

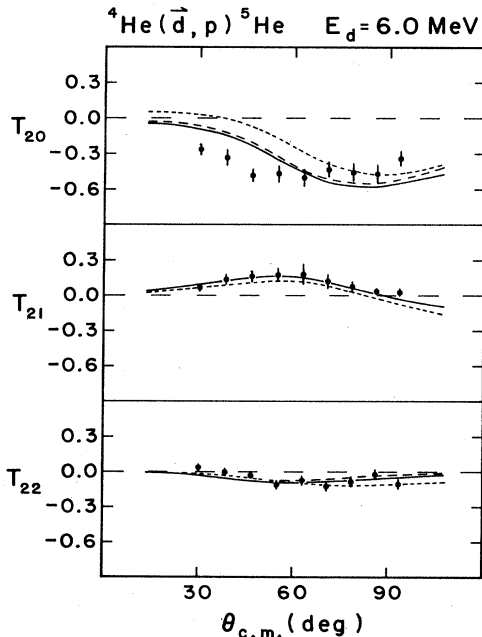


FIG. 12. The tensor analyzing powers for the ${}^4\text{He}(d,p){}^5\text{He}(\text{g.s.})$ reaction as a function of the proton center-of-mass angle at $E_d=6.0$ MeV. The curves are the result of three-body calculations which are described in the caption for Fig. 3.

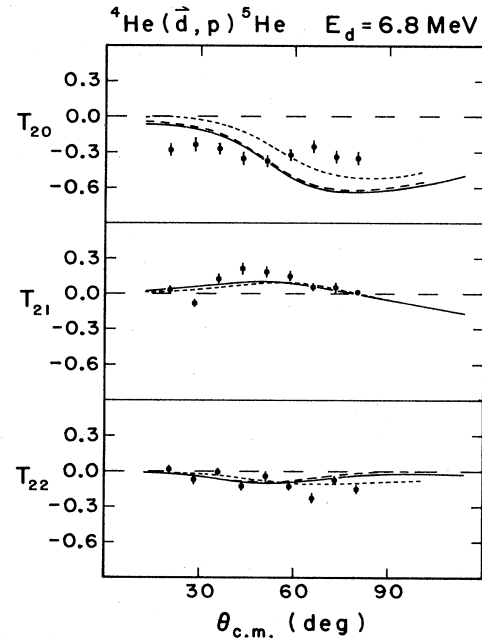


FIG. 13. The tensor analyzing powers for the ${}^4\text{He}(d,p){}^5\text{He}(\text{g.s.})$ reaction as a function of the proton center-of-mass angle at $E_d=6.8$ MeV. The curves are the result of three-body calculations which are described in the caption for Fig. 3.

Therefore it appears that both Coulomb effects and the 1^+ resonance are of importance in this energy region. The discrepancies between the calculations and the data are also largest at the lowest energies. Part of this may result from the failure of the calculations to correctly include Coulomb effects, as noted above, but the calculations may also not adequately describe effects of the 1^+ resonance as well. Although the nucleon-alpha potential used in the calculations reproduces the nucleon-alpha scattering phase shifts well, the off-shell behavior of the two-body T matrix may be less well described, and this will affect the three-body part of the 1^+ resonance wave function.

The ${}^4\text{He}(d,p){}^4\text{He}$ reaction may be considered a good vehicle for the study of the ${}^6\text{Li}$ 1^+ resonance. Two other resonances which might contribute to the breakup process exist in this energy range. These are the $J^\pi=0^+$, $T=1$ and $J^\pi=2^+$, $T=0$ states in ${}^6\text{Li}$. From isospin conservation the 0^+ resonance is not expected to contribute strongly to the breakup.¹⁵ The 2^+ resonance is an unlikely candidate as well, if one considers the sign of the T_{20} analyzing power, since the formation of ${}^6\text{Li}$ in the 2^+ state preferentially involves deuterons having their spins aligned perpendicularly to the normal to the reaction plane, which corresponds to $T_{20} > 0$. Therefore, if the 1^+ resonance is playing a large part in the breakup process, as the calculations indicate, its effect as manifested in the energy dependence of the analyzing powers is different from that predicted by the calculations. However, the variation in iT_{11} for the ${}^5\text{He}$ ground state as a function of bombarding energy (Figs. 9 and 10) presents good evidence for the effect of the 1^+ resonance on the breakup.

CONCLUSIONS

The considerable difference between measured and calculated iT_{11} at 5.4 MeV indicates strong Coulomb effects which are not being fully accounted for in the theory. However, these presumed Coulomb effects cannot be separated from what also appear to be resonance effects. Certainly a better treatment of the Coulomb interaction in the three-body calculations would be helpful in clarifying the role played by the resonance.

Discrepancies between data and calculations are quite evident for T_{20} in Figs. 11–13. This is not completely unexpected, as the three-body calculations have also had difficulty in reproducing T_{20} at higher energies.¹⁰ The problem is still not well understood, but may be related to the off-shell dependence of the n - α T matrix mentioned above. The effect of the 1^+ resonance is also not as pronounced in the data as in the calculations. This is consistent with a phase-shift analysis¹⁶ of d - α scattering, which shows the 1^+ absorption parameter to be smaller

than that predicted by the three-body calculations.

The results presented here clearly indicate the need for the tensor interaction in the calculations. With the exception of the iT_{11} data for $\theta_{c.m.}=90^\circ$ shown in Fig. 10, calculations including the tensor interaction are at least qualitatively in closer agreement with the data than those which omit this interaction.

In summary, we have measured cross sections and all four analyzing powers for the inclusive breakup reaction ${}^4\text{He}(d,p)n{}^4\text{He}$ at bombarding energies near the 1^+ resonance in ${}^6\text{Li}$. Comparisons between polarization data for the formation of the ${}^5\text{He}$ ground state and three-body calculations show the effects of this resonance and Coulomb interference on the breakup. The three-body calculations, while not giving a complete description of the breakup process, provide a good overall description of this reaction in the energy region of the ${}^6\text{Li}$ resonance.

This work was supported in part by the National Science Foundation under Contract No. PHY82-00426.

*Present address: AT&T Bell Laboratories, Holmdel, NJ 07733.

†Present address: Emory and Henry College, Emory, VA 24327.

¹P. E. Shanley, Phys. Rev. **187**, 132B (1969).

²B. Charnomordic, C. Fayard, and G. H. Lamot, Phys. Rev. C **15**, 864 (1977).

³Y. Koike, Prog. Theor. Phys. **59**, 87 (1978).

⁴Y. Koike, Nucl. Phys. **A301**, 411 (1978).

⁵Y. Koike, Nucl. Phys. **A337**, 23 (1980).

⁶H. D. Knox, R. G. Graves, F. N. Rad, M. L. Evans, L. C. Northcliffe, H. Nakamura, and H. Noya, Phys. Lett. **56B**, 33 (1975).

⁷H. Nakamura, N. Noya, S. E. Darden, and S. Sen, Nucl. Phys. **A305**, 1 (1978).

⁸I. Slaus, J. M. Lambert, P. A. Treado, F. D. Correll, R. E. Brown, R. A. Hardekopf, N. Jarmie, Y. Koike, and W. Grüebler, Nucl. Phys. **A397**, 205 (1983).

⁹M. Bruno, F. Cannata, M. D'Agostino, B. Jenny, W. Grüebler,

V. König, P. A. Schmelzbach, and P. Doleschall, Nucl. Phys. **A407**, 29 (1983).

¹⁰M. Ishikawa, S. Seki, K. Foruno, Y. Tagishi, M. Sawada, T. Sugiyama, K. Matsuda, M. Morayama, N. X. Dai, J. Sanada, and Y. Koike, Phys. Rev. C **28**, 1884 (1983).

¹¹H. Oswald, M. Buballa, J. Helten, M. Karus, B. Laumann, R. Melzer, P. Niessen, G. Rauprich, J. Schulte-Uebbing, H. Paetz gen. Schieck, and Y. Koike, Nucl. Phys. **A435**, 77 (1985).

¹²R. R. Cadmus, Jr. and W. Haerberli, Nucl. Instrum. Methods **129**, 403 (1973).

¹³L. G. Keller and W. Haerberli, Nucl. Phys. **A172**, 625 (1968).

¹⁴H. Oswald, W. Burgmer, D. Gola, C. Heinrich, H. J. Helten, H. Paetz gen. Schieck, and Y. Koike, Phys. Rev. Lett. **46**, 307 (1981).

¹⁵C. Wernitz and F. Cannata, Phys. Rev. C **24**, 349 (1981).

¹⁶B. Jenny, W. Grüebler, V. König, P. Schmelzbach, and C. Schweizer, Nucl. Phys. **A397**, 61 (1983).